J. Earth Planet. Sci. Nagoya Univ., Vol. 54, 1 to 12, 2007

Reexamination of CHIME monazite ages for granite samples from Wugongshan and Huangshan, southeastern China

Kazuhiro SUZUKI[1], Izumi KAJIZUKA[1], Dezi WANG[2] and Kanenori SUWA[3]

[1]*Chronological Research Center, Nagoya University, Nagoya 464-8602, Japan*
[2]*Department of Earth Sciences and State Key Laboratory for Mineral Deposits Research, Nanjing University, 210093 Nanjing, People's Republic of China*
[3]*Professor Emeritus of Nagoya University, Department of Earth and Planetary Sciences, School of Science, Nagoya University, Nagoya 464-8602, Japan*
(Received December 11, 2007 / Accepted December 27, 2007)

ABSTRACT

The ages of granite samples from Wugongshan and Huangshan, southeastern China were reexamined with the CHIME method coupled with screening of possibly concordant monazite analyses by the chemical criterion that $0.95<(Ca+Si)/(Th+U+Pb+S)<1.05$. The age mapping technique reveals that monazite grains in sample Wugongshan-2, K-feldspar porphyritic muscovite-biotite granite, are chronologically zoned with the dominant central domain. The CHIME ages are 159±12 Ma for the central domain and 129±14 Ma for the marginal domain. Sample Wugongshan-3, coarse-grained peraluminous muscovite-biotite granite, gives a 164±19 Ma monazite age. The CHIME monazite ages for samples Huangshan-9 and -10, within-plate type muscovite-bearing biotite granites, are 130±19 and 138±6 Ma, respectively. Previous CHIME monazite ages, 173±10 Ma for Wugongshan samples and 162±10 Ma for Huangshan samples (Suzuki *et al.*, 2000), appear to have resulted from mixing of concordant and discordant datasets and/or datasets for different age domains. The revised CHIME monazite ages provide chronological constraint for the tectonic evolution of southeastern China including the change from a subduction-related compressive environment to an extensional environment.

INTRODUCTION

One of the authors (D.Z. Wang) donated many hand specimens of granitic rocks from southeastern China to Nagoya University, when he was invited to Nagoya University as a JSPS visiting professor in 1986. The samples are housed in Department of Earth Sciences and subsequently in the Nagoya University Museum; they have been used for petrographic training of the undergraduate course as well as advanced research works.

Among the granite samples, those from Wugongshan and Huangshan were dated to be of middle Jurassic (173±10 Ma for monazite in Wugongshan samples and 162±10 Ma for monazite in Huangshan samples, Suzuki *et al.*, 2000) through the CHIME method (Suzuki and Adachi, 1991). The CHIME monazite ages are inconsistent with the current view that most granitic rocks in these areas are of Indosinian and late Yanshanian (226-259 Ma and 100–130 Ma K-Ar ($^{40}Ar/^{39}Ar$) ages, respectively) according

to Faure *et al.* (1996) and Li (2000). Some may consider that the CHIME ages are questionable, because the dating method does not appear to provide information about discordancy in the Th-U-Pb system. During the subsequent work of CHIME dating, it has become obvious that the apparent ages are more variable in monazite with the (Ca+Si)/(Th+U+Pb+S) ratio deviated largely from unity than in monazite with the ratio close to unity (Sun and Suzuki, 2004; Suzuki and Kato, in press). This chemical criterion can possibly discriminate monazite analyses on possibly concordant domains from those on discordant domains. Suzuki *et al.* (2000) did not measure Ca, Si and S at the dating of monazite in Wugongshan and Huangshan samples; it is hard to ascertain the reliability of the 173±10 and 162±10Ma ages. We, therefore, reexamine monazites in the Wugongshan and Huangshan samples.

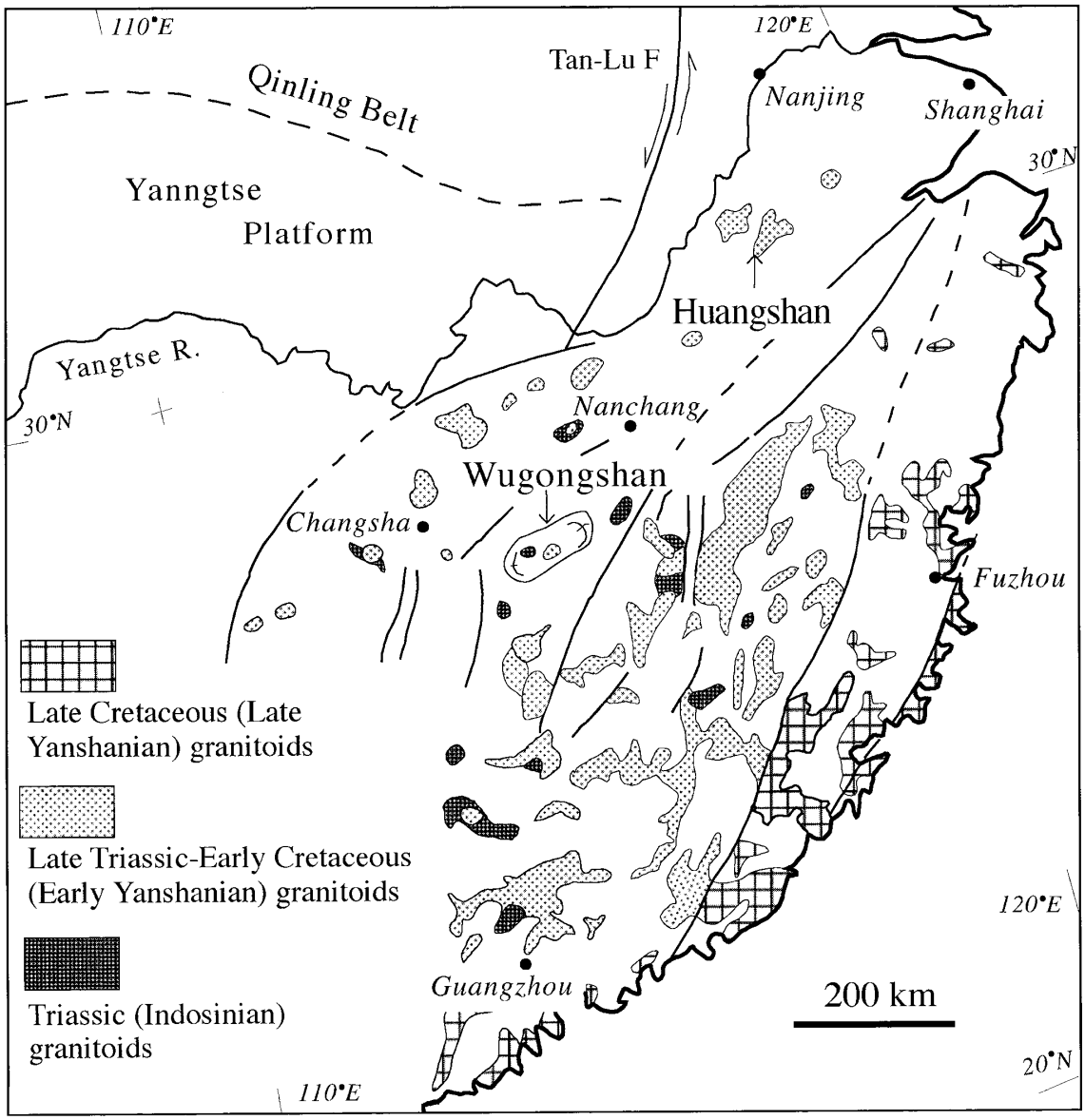

Fig. 1 Locations of Wugongshan and Huangshan in the structural map of southeastern China with distribution of the Indosinian and Yanshanian granitoids (simplified from Faure *et al.*, 1996).

GEOLOGY AND SAMPLE DESCRIPTIONS

The geology of southeastern China is characterized by the extensive Indosinian (Permian-Triassic) and Yanshanian (Jurassic-Cretaceous) plutonisms (Fig. 1). The early Yanshanian (Jurassic) plutonism is dominated by peraluminous S-type granitoids at 164–153 Ma, and the late Yanshanian (Cretaceous) plutonism is dominated by high-K I-type and A-type granitoids with ages of 146–136 Ma, 129–122 Ma, 109–101 Ma and 97-87 Ma (Li, 2000).

Wugongshan is situated at 26°29′N and 115°37.5′E. The area presents a dome structure and is underlain by Paleozoic metamorphic basements, Caledonian Shanzhuang granodiorite and Yanshanian granitoids (Wang *et al.*, 2001). The Yanshanian granitoids show a geochemical affinity of peraluminous S-type granite. They are characterized by high SiO_2 (71.7–74.7 wt.%), K_2O+Na_2O (7–9 wt.%) and K_2O/Na_2O (1.1–2.0) (Wang *et al.*, 2001).

Granite sample Wugongshan-2, described originally as migmatite, is characterized by the presence of K-feldspar phenocrysts of 2–3 cm in length, and consists mostly of quartz, microcline, plagioclase and biotite with subordinate amounts of muscovite. Plagioclase is partly replaced by fine-grained secondary muscovite. Accessory minerals include zircon, apatite, ilmenite and monazite. Granite sample Wugongshan-3 is

Table 1 XRF analyses of granitic rocks from Wugongshan and Huangshan, southeastern China.

	Wugongshan		Huangshan	
	2	3	9	10
SiO_2 (wt.%)	70.7	71.0	74.8	73.5
TiO_2	0.28	0.24	0.10	0.08
Al_2O_3	15.0	14.8	12.4	13.4
FeO	1.99	1.59	1.43	1.47
MnO	0.05	0.04	0.04	0.03
MgO	0.42	0.35	0.05	0.03
CaO	1.28	1.01	0.67	0.83
Na_2O	2.81	3.11	3.40	3.84
K_2O	6.33	5.53	4.28	4.77
P_2O_5	0.13	0.16	0.02	0.01
Total	98.99	97.83	97.19	97.96
V (ppm)	23.8	14.3	3.5	2.2
Cr	12.0	15.4	13.9	11.9
Co	4.1	2.7	2.9	2.6
Ni	3.4	6.2	8.0	5.9
Zn	41.7	55.3	54.8	29.8
Rb	349	405	583	485
Sr	121	79.8	2.4	13.2
Y	28.7	24.7	122	145
Zr	143	148	151	154
Nb	1.2	2.6	43.9	31.3
Ba	570	360	90	140
Pb	39.6	38.3	24.8	36.2
Th	22.3	32.4	55.5	50.5

coarse-grained massive two-mica granite. Most plagioclase grains in this sample show weak alteration. Accessory minerals are zircon, apatite, ilmenite and monazite. The XRF analyses are listed in Table 1. Both samples are chemically similar to each other and characterized by high K_2O (6.33 and 5.53 wt.%), K_2O+Na_2O (9.14 and 8.64 wt.%), K_2O/Na_2O (2.25 and 1.78) and Al/(Na+K+2Ca) (1.09 and 1.14). The Rb concentrations, 349 and 405 ppm, are compatible with those of the Yanshanian granites within the Wugongshan dome (Lou *et al.*, 2006), but the present samples appear to be less evolved than rocks described by Lou *et al.* (2006).

Huangshan is 1864-m high and situated at 30°10′N and 118°11′E, south of the lower reaches of the Changjiang River. It consists of biotite granite with plagioclase, albite or Na-rich oligoclase and quartz, and biotite is interstitial to feldspars and quartz. Chemical composition is characterized by high concentrations of SiO_2, Na_2O+K_2O, Y, Nb and Zr and low concentrations of CaO, MgO, Sr and Ba. The characteristics of the Huangshan massif are very different from those of I- and S-type granites in southern China, but are quite similar to those of A2-type granites (Jiang *et al.*, 1999).

Granite sample Huangshan-9 is medium-grained and Huangshan-10 is coarse-grained. They consist mainly of albite to albitic oligoclase, microcline-perthite and quartz. Subordinate amounts of biotite form aggregates in Huangshan-9 and are interstitial to main constituents. Muscovite occurs as an interstitial phase in both samples. Accessory minerals include apatite, zircon, magnetite, ilmenite, thorite and monazite. Magnetite disperses in biotite aggregates in Huangshan-9. Both samples show high concentrations of SiO_2 (74.8 and 73.5 wt.%), Na_2O+K_2O (7.68 and 8.61 wt.%), Rb (583 and 485 ppm) and low concentrations of MgO (0.05 and 0.03 wt.%), CaO (0.67 and 0.83 wt.%), Sr (2.4 and 13.2 ppm) and Ba (90 and 140 ppm) (Table 1). The Zr concentrations (151 and 154 ppm) appear to be high compared with those of normal evolved S- and I-type granites. These chemical features accord with those for granites described by Jiang *et al.* (1999). The high concentrations of Y (122 and 145 ppm) and Nb (43.9 and 31.3 ppm) coupled with the high Rb concentrations suggest a within-plate granite character of Pearce *et al.* (1984). Further, the geochemical signatures, such as high Zr + Nb + Y, Zr/Ni and Rb/Sr, are quite similar to those of the A-type granite characteristics (Whalen *et al.*, 1987).

CHIME DATING

Monazite grains in polished thin sections were analyzed by using the JEOL JCXA-733 electron microprobe that was equipped with 4 wavelength dispersive spectrometers with a 140 mm radius of the Rowland circle. Individual spectrometers were equipped with a PET (002 pentaerythritol) diffraction crystal and a sealed Xe X-ray detector. Instrument operating conditions for the spot by spot analysis were 15 kV accelerating voltage, 3 μm probe diameter and 150 nA probe current. ThMα, UMβ, PbMα and YLα lines were measured simultaneously, and CaKα, SKα, PKα, SiKα, KKα and NbLα lines were also measured. For the analyses of Th, U, Pb and Y, X-ray intensity was integrated over 400s period for the line peak position and over 200s period for two optimum background positions. To ensure that possible changes of the sample surface had a minimal effect on the results, the measurement of peak and background

positions was repeated five times for each analysis. For the analyses of other elements, X-ray intensities were integrated over 40s on each line peak position and 20s on two background positions. The background value for each line was estimated by exponential fitting of two readings. The standards were euxenite provided by Smellie *et al.* (1978) for Th, U and Nb, synthesized glass (Suzuki and Adachi, 1998) for Pb, Si and Ca, synthesized Y-glass (Y_2O_3= 10 wt% and K_2O= 2 wt%) for Y and K, barite for S and xenotime for P. A high Th monazite with little U was used to determine the X-ray interference correction factors. The interferences of ThMγ, ThM3-N4 and ThM5-P3 lines on UMβ and $NbL\beta_3$, YLγ, ThMζ and sSKα lines on PbMα were corrected through the procedures described in Suzuki and Kato (in press). The X-ray intensity data were converted into concentrations by the Bence and Albee's method (Bence and Albee, 1968) using the α-factor table provided by Kato (2005) and analyses of natural minerals as the matrix composition. The small difference in the matrix between analyzed and reference minerals has a negligible effect on the ThO_2, UO_2 and PbO determinations. The detection limits at a 2σ confidence level were 0.009, 0.011 and 0.006 wt.% for ThO_2, UO_2 and PbO, respectively. Relative errors were about 10% for 0.03 wt.% PbO, 2% for 0.6 wt.% UO_2 and 0.5% for 7.0 wt.% ThO_2.

For the age mapping, probe current and probe diameter were 400 nA and 2 μm, respectively. The dwell time was 10s for the line peak measurement and 5s for the background measurement. The pixel step was 2 μm. The raw intensity data were first corrected for background and interferences of ThMγ, ThMζ and YLγ, and then converted into concentration in the same way as the spot by spot analysis. Apparent ages of individual spots were calculated by assuming no initial Pb by equation (1) of Suzuki and Adachi (1991).

RESULTS

The compositional and age maps of M01 monazite grain in Wugongshan-2 are given in Fig. 2. The spot by spot analyses are listed in Table 2, and the PbO vs. ThO_2* relationships are illustrated in Fig. 3.

Monazite grain M01 in Wugongshan-2 is included in biotite and shows an irregular shape of about 0.1 mm in size (Fig. 2). The ThO_2 content ranges from 7.0 to 16.5 wt.% and the UO_2 content from 0.2 to 0.6 wt.%. The ThO_2 and UO_2 contents are covariant with each other in the left of the grain, but in the right of the grain they are variable. The Y_2O_3 content ranges from 0.8 to 2.5 wt.%. The PbO content is as high as 0.15 wt.%. It appears to be generally covariant with the ThO_2 and UO_2 contents, but significant depletion was recognized at the upper-left and lower-right. The age map shows that the monazite grain consists mainly of c. 160 Ma central domain with older islands and c. 130 Ma marginal domain.

Within monazite structure ($LREEPO_4$ where LREE represents light rare earth elements), main of substitution components are $ThSiO_4$ (huttonite; LREEP=ThSi), $CaTh(PO_4)_2$ (bravandite: 2LREE=CaTh), YPO_4 and $CaSO_4$. The (Ca+Si)/(Th+U+Pb+S) ratio becomes a temporal criterion for discordance of the Th-U-Pb system (Sun and Suzuki, 2004; Suzuki and Kato, in press). The large deviation in the (Ca+Si)/(Th+U+Pb+S) ratios is encountered for spots on metamict portions as well as for

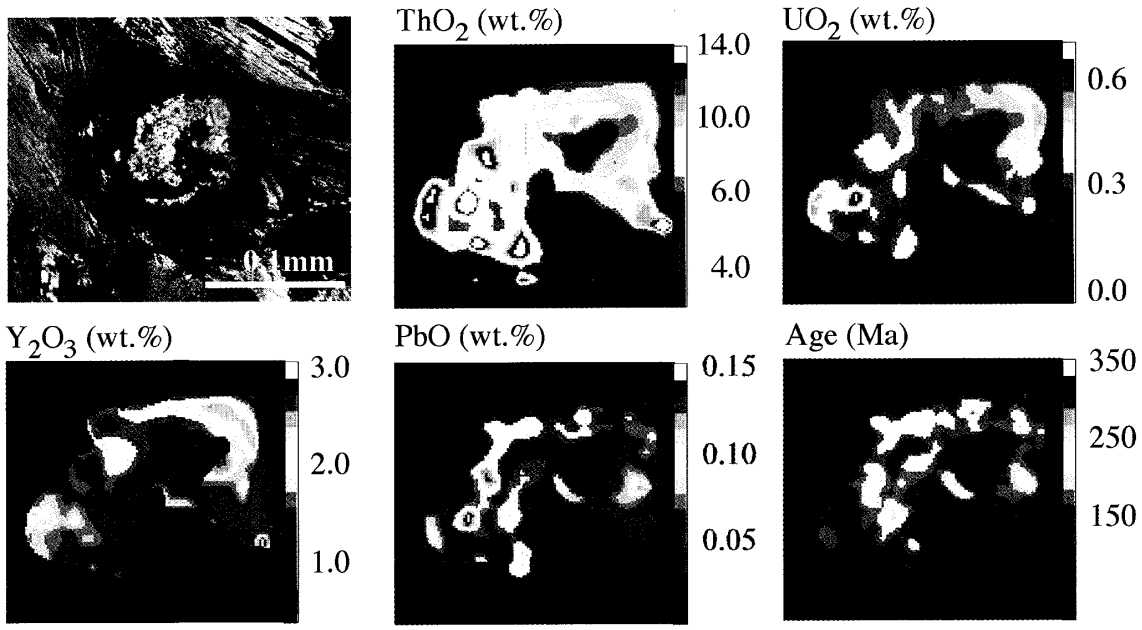

Fig. 2 Photomicrograph (crossed polars), compositional maps and a chronological map for M01 monazite grain in Wugongshan-2 granite sample.

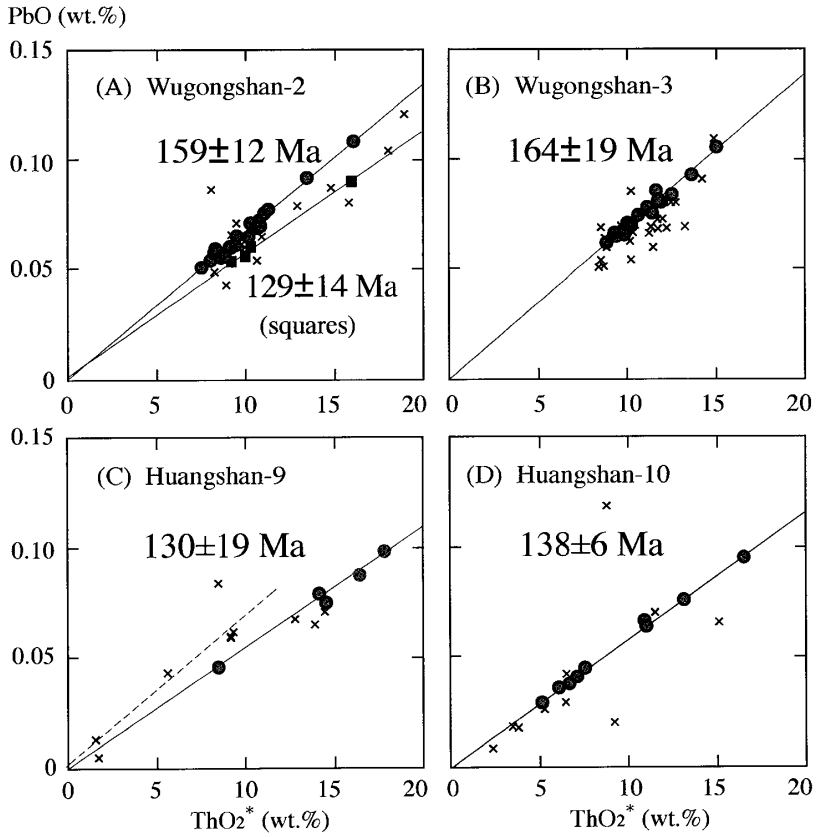

Fig. 3 PbO-ThO_2* plots for analyzed monazites in Wugongshan-2 (A), Wugongshan-3 (B), Huangshan-9 (C) and Huangshan-10 (D) samples. Filled circles represent data points screened by the criterion of 0.95< (Ca+Si)/(Th+U+Pb+S)<1.05 and crosses show data points rejected by the criterion. Filled squares in (A) represent screened data points on the marginal domain. Broken line in (C) is 160 Ma reference isochron.

Table 2 Partial electron microprobe analyses of monazite in granitic rocks from Wugongshan and Huangshan, southeastern China. Age: apparent age in Ma, ThO_2*: measured ThO_2 plus ThO_2 equivalent of the measured UO_2, R: the molar $(CaO+SiO_2)/(ThO_2+UO_2+PbO+S)$ ratio, "-": below detection limit, ○: screened data for the central domain, and □: screened data for the marginal domain.

Spot No.	ThO_2	UO_2	PbO	Age	ThO_2*	CaO	Y_2O_3	S	K_2	SiO_2	R
Wugongshan-2											
M01-01○	7.04	0.343	0.0577	167	8.15	0.628	1.29	–	0.007	1.00	0.99
M01-02○	9.76	0.337	0.0697	152	10.8	0.892	1.03	0.005	0.008	1.38	1.01
M01-03	7.82	0.331	0.0433	115	8.88	2.01	0.88	0.004	0.008	1.66	2.04
M01-04	16.5	0.466	0.1042	137	18.0	0.819	1.01	0.006	0.012	3.42	1.10
M01-05	14.4	0.432	0.0806	120	15.8	1.04	0.85	–	0.018	3.52	1.36
M01-06○	7.73	0.405	0.0603	158	9.04	0.974	1.74	–	0.012	0.86	1.02
M01-07	8.72	0.361	0.0604	145	9.88	0.671	1.05	–	0.013	1.48	1.06
M01-08○	8.63	0.531	0.0713	163	10.3	1.17	1.77	–	0.021	0.87	1.01
M01-09○	9.15	0.443	0.0706	158	10.6	0.688	1.26	–	0.022	1.53	1.03
M01-10	9.35	0.337	0.0650	147	10.4	0.829	1.02	–	0.016	1.63	1.13
M02-01○	7.39	0.284	0.0589	168	8.31	0.461	0.94	–	0.023	1.26	1.00
M02-02○	9.66	0.303	0.0688	153	10.6	0.736	0.95	–	0.029	1.48	0.99
M02-03○	8.56	0.265	0.0609	153	9.41	0.702	0.88	–	0.018	1.29	1.01
M02-04○	8.52	0.291	0.0654	164	9.46	0.703	0.95	–	0.031	1.33	1.03
M02-05○	7.81	0.299	0.0562	152	8.77	0.488	0.98	–	0.030	1.35	1.01
M02-06○	9.15	0.290	0.0651	153	10.1	0.663	0.81	–	0.025	1.44	0.99
M02-07○	9.97	0.369	0.0776	164	11.2	0.476	1.01	–	0.031	1.86	1.00
M03-01○	9.45	0.378	0.0725	161	10.7	0.433	0.97	–	0.022	1.74	0.98
M03-02○	9.80	0.385	0.0756	162	11.0	0.469	1.03	–	0.035	1.80	0.99
M03-04□	9.15	0.258	0.0554	131	9.98	0.640	0.74	–	0.007	1.46	0.99
M03-05□	8.58	0.203	0.0515	132	9.24	0.718	0.63	–	0.009	1.29	1.02
M03-06○	8.61	0.479	0.0713	166	10.2	1.42	0.91	–	0.010	0.50	0.97
M04-01	7.32	0.288	0.0491	141	8.24	0.891	1.02	–	0.020	1.96	1.67
M04-02○	12.4	1.13	0.1085	160	16.0	0.737	1.35	–	0.027	2.43	1.04
M04-03○	9.92	1.07	0.0918	162	13.4	0.780	1.41	–	0.009	1.62	0.97
M04-04	11.4	1.04	0.0879	141	14.8	0.747	1.36	–	0.020	2.22	1.06
M04-05	7.52	0.622	0.0714	177	9.52	0.655	1.34	–	0.014	1.89	1.39
M04-06	7.96	0.478	0.0600	149	9.49	1.18	1.34	–	0.016	1.54	1.45
M04-07	16.8	0.638	0.1211	152	18.9	9.329	0.74	0.011	0.026	4.96	3.72
M04-08	8.39	0.778	0.0652	142	10.9	0.753	1.12	–	0.012	1.67	1.18
M04-09	8.69	0.610	0.0546	121	10.6	1.56	0.95	–	0.011	2.36	1.90
M04-10□	12.3	1.12	0.0910	136	15.9	0.624	1.12	–	0.019	2.36	0.99
M04-11	10.7	0.705	0.0791	145	12.9	0.588	1.27	0.005	0.015	2.74	1.29
M04-12	6.16	0.579	0.0869	255	8.04	0.963	1.18	–	0.005	2.01	1.96
M05-01○	7.90	0.381	0.0599	155	9.12	0.725	1.27	–	0.042	1.11	0.99
M05-02□	8.73	0.472	0.0576	133	10.2	0.808	1.44	–	0.043	1.23	1.00
M06-01○	7.19	0.239	0.0542	161	7.96	0.433	0.69	–	0.024	1.27	1.02
M06-02○	6.71	0.232	0.0509	161	7.46	0.445	0.60	–	0.029	1.18	1.04
M06-03○	7.25	0.308	0.0594	170	8.25	0.667	1.08	–	0.045	1.04	1.01
M06-04	8.26	0.297	0.0661	170	9.22	0.547	0.69	–	0.090	1.92	1.27
M07-01○	7.89	0.214	0.0556	153	8.58	0.547	0.70	–	0.029	1.20	0.96

Table 2 (continued)

Spot No.	ThO_2	UO_2	PbO	Age	ThO_2*	CaO	Y_2O_3	S	K_2	SiO_2	R
Wugongshan-3											
M01-01	7.93	0.294	0.0607	162	8.88	1.44	0.92	0.107	0.101	1.16	1.30
M02-01	9.50	0.368	0.0762	169	10.7	1.70	1.05	0.004	0.113	0.83	1.17
M03-01○	9.39	0.147	0.0661	159	9.86	1.12	0.44	–	0.024	0.97	0.99
M03-02○	9.04	0.124	0.0658	165	9.44	1.05	0.43	–	0.022	0.90	0.96
M03-03○	8.13	0.629	0.0712	166	10.2	1.51	1.28	–	0.025	0.48	1.04
M03-04○	9.10	0.140	0.0676	167	9.55	1.03	0.42	–	0.014	0.99	0.99
M04-01	8.36	0.593	0.0678	156	10.3	1.45	0.93	–	0.396	11.5	6.35
M05-01	8.48	0.602	0.0717	163	10.4	1.55	1.01	–	0.082	1.17	1.36
M05-02	7.80	0.236	0.0704	194	8.56	0.986	0.82	0.005	0.142	1.86	1.57
M06-01○	9.91	0.805	0.0845	160	12.5	2.00	2.36	–	0.030	0.33	1.00
M06-02○	9.60	0.710	0.0809	161	11.9	1.90	2.20	–	0.043	0.35	1.01
M07-01	7.58	0.382	0.0626	168	8.81	0.930	0.77	0.003	0.036	0.83	1.80
M08-02	10.4	0.674	0.0808	152	12.6	2.29	1.88	–	0.029	1.32	1.48
M09-01	7.98	0.824	0.0479	107	10.6	1.48	0.66	–	1.85	6.99	4.26
M10-01	8.82	1.40	0.0705	125	13.3	1.96	1.29	0.006	0.203	1.48	1.52
M11-01	7.95	0.160	0.0520	145	8.46	1.11	0.37	–	0.061	4.24	2.92
M11-02	8.73	1.21	0.0815	153	12.6	1.81	1.89	–	1.58	5.87	3.43
M11-03	8.93	0.916	0.0727	145	11.9	1.88	2.33	–	0.075	0.26	1.01
M11-04	9.01	0.981	0.0692	135	12.2	1.91	2.29	–	0.100	0.31	1.03
M12-01	4.15	2.05	0.0404	89	10.7	0.884	0.59	0.010	0.282	2.40	2.34
M12-02	7.89	0.669	0.0677	159	10.0	1.60	1.92	–	1.10	9.79	5.86
M13-01	10.2	1.25	0.0920	153	14.2	2.29	2.00	–	0.088	0.37	1.08
M13-02○	11.1	0.777	0.0934	163	13.6	2.23	2.24	–	0.020	0.31	0.99
M13-03	6.98	1.48	0.0693	139	11.8	1.45	1.43	–	2.31	9.22	5.56
M14-01	5.45	1.50	0.0550	127	10.3	1.30	0.69	–	2.72	11.2	7.83
M15-01	7.84	0.256	0.0530	145	8.67	1.41	0.56	0.011	0.023	4.48	3.19
M16-01	9.36	0.587	0.0675	142	11.3	1.84	1.21	–	0.281	1.49	1.52
M17-01	8.08	0.143	0.0551	153	8.54	1.19	0.37	0.004	0.056	0.71	1.05
M17-02○	9.30	0.281	0.0655	152	10.2	1.45	0.93	–	0.048	0.75	1.04
M18-01	11.2	0.242	0.0741	147	12.0	1.78	1.06	0.003	0.022	1.10	1.15
M19-01	10.4	0.348	0.0608	125	11.5	3.34	1.08	0.010	0.013	0.73	1.74
M19-02○	10.7	0.331	0.0826	166	11.8	1.95	0.92	–	0.017	0.45	1.00
M19-03○	10.4	0.311	0.0762	158	11.4	1.94	1.07	–	0.025	0.49	1.04
M19-04	10.3	0.333	0.0698	145	11.4	2.01	1.02	–	0.031	0.55	1.11
M19-05○	10.7	0.316	0.0820	165	11.7	1.92	0.86	–	0.019	0.56	1.03
M20-01	6.89	0.601	0.0646	173	8.83	1.52	0.89	0.014	0.557	2.54	2.39
M21-01	10.7	1.29	0.1102	175	14.9	2.38	2.34	–	0.083	0.45	1.09
M21-02○	9.32	1.77	0.1063	168	15.0	2.19	2.20	–	0.041	0.22	1.01
M23-01	9.36	0.301	0.0866	198	10.3	1.91	1.27	0.006	0.027	1.32	1.51
M24-01○	9.30	0.223	0.0715	169	10.0	1.58	0.70	–	0.043	0.54	1.02
M24-02○	10.4	0.297	0.0779	163	11.3	1.76	1.01	–	0.045	0.52	0.98
M24-03○	10.6	0.309	0.0866	177	11.6	1.75	0.97	–	0.024	0.69	1.03
M24-04○	8.72	0.212	0.0654	164	9.40	1.54	0.78	–	0.036	0.45	1.02
M24-05○	8.58	0.224	0.0670	170	9.30	1.54	0.73	–	0.038	0.42	1.03
M24-06○	9.83	0.239	0.0751	168	10.6	1.70	0.79	–	0.034	0.52	1.01
M24-07○	10.0	0.316	0.0787	168	11.1	1.69	1.07	–	0.040	0.52	0.98

Table 2 (continued)

Spot No.	ThO_2	UO_2	PbO	Age	ThO_2*	CaO	Y_2O_3	S	K_2	SiO_2	R
Huangshan-9											
M01-01	9.78	1.28	0.0659	112	13.9	0.324	1.90	0.008	0.058	2.37	1.07
M04-01	7.42	0.324	0.0844	236	8.47	20.3	0.58	0.004	0.054	3.30	2.03
M04-02	11.3	0.473	0.0682	126	12.8	0.213	1.13	–	0.081	3.37	1.34
M04-03	8.18	0.329	0.0599	153	9.24	1.00	1.00	–	0.087	1.30	1.21
M05-01○	12.1	0.609	0.0792	133	14.1	0.126	1.23	–	0.040	2.80	1.01
M05-02	12.3	0.662	0.0715	117	14.5	0.102	1.16	–	0.059	3.14	1.09
M05-03○	12.5	0.618	0.0752	123	14.5	0.097	1.26	–	0.036	2.93	1.01
M05-04	8.29	0.299	0.0600	153	9.25	0.118	0.39	–	0.091	2.01	1.09
M09-01	1.33	0.073	0.0141	212	1.57	0.437	1.36	–	0.042	0.23	2.15
M09-02	1.46	0.085	–	–	–	0.317	1.43	–	0.036	0.29	1.80
M09-03	1.48	0.082	0.0055	75	1.74	0.434	1.68	–	0.027	0.24	1.98
M11-01○	14.8	0.488	0.0880	127	16.4	0.123	1.69	–	0.027	3.39	1.00
M11-02○	15.6	0.690	0.0984	131	17.8	0.105	1.78	–	0.020	3.59	0.99
M11-03○	7.73	0.230	0.0460	128	8.47	1.03	1.00	–	0.025	0.74	1.01
M11-04	4.80	0.263	0.0440	184	5.64	0.703	0.93	–	0.182	1.81	2.21
Huangshan-10											
M02-01	1.87	0.169	0.0090	88	2.41	0.452	1.61	–	0.071	0.36	1.80
M03-01○	15.1	0.437	0.0956	137	16.5	0.161	0.16	0.004	0.014	3.30	0.97
M03-02○	9.91	0.317	0.0666	144	10.9	0.157	0.13	–	0.023	2.13	0.98
M03-03	13.8	0.427	0.0664	104	15.1	0.370	5.07	0.005	0.028	3.11	1.08
M05-01	9.91	0.479	0.0707	146	11.5	0.109	0.81	0.004	0.155	2.99	1.30
M05-02	5.93	0.183	0.0431	156	6.52	0.132	0.19	0.003	0.050	1.75	1.34
M05-03	8.01	0.247	0.1190	319	8.81	0.188	1.63	–	0.037	2.29	1.30
M05-04○	11.6	0.481	0.0762	138	13.1	0.109	1.39	0.003	0.028	2.58	0.98
M06-01○	9.67	0.416	0.0641	138	11.0	0.131	0.99	–	0.042	2.28	1.04
M07-01○	4.45	0.200	0.0297	138	5.10	0.091	0.44	–	0.027	0.99	1.02
M07-02	3.94	0.418	0.0268	120	5.28	0.121	0.40	–	0.388	1.30	1.43
M07-03○	5.28	0.238	0.0362	142	6.05	0.046	0.30	–	0.012	1.24	1.02
M07-04○	5.88	0.251	0.0380	134	6.69	0.039	0.29	–	0.013	1.38	1.02
M07-05○	6.30	0.258	0.0410	136	7.13	0.041	0.28	–	0.009	1.46	1.00
M07-06○	6.65	0.275	0.0454	142	7.54	0.052	0.43	0.006	0.017	1.52	0.99

spots on grain margin and close to inclusions, veins and fractures. These spots show occasionally a significant concentration of K that is hard to be incorporated into monazite structure. Datasets with $0.95<(Ca+Si)/(Th+U+Pb+S)<1.05$ are selected for the CHIME age calculation. The screened datasets are marked with open circles in Table 2. The screened datasets for the marginal domains of monazite grains in Wugongshan-2 are marked with open squares.

Wugongshan-2: A total of 41 spots on 7 grains were analyzed, and 26 datasets passed through the chemical criterion. M04-12 represents an old island within the central domain. The (Ca+Si)/(Th+U+Pb+S) ratio is 1.96. The analyzed islands in the central domain can be assumed to be discordant. This, however, does not exclude the possibility that islands inherited old monazite. The screened datasets for the central domain (marked by open circles in Table 2) give 150–170 Ma apparent ages,

and those for the marginal domain (marked by open squares in Table 2) give c. 130 Ma apparent ages. The PbO versus ThO_2* plot is shown in Fig. 3A. Data points for the central domain of individual monazite grains (filled circles) define an isochron of 159±12 Ma (MSWD=0.25) with an intercept value of 0.0004±0.0054, and those for the marginal domain (small filled squares) give an isochron of 129±14 Ma with an intercept value of 0.0033±0.0067.

Wugongshan-3: Monazite grains in this sample are generally smaller than 0.02 mm in size. Most analyses show high concentrations of CaO, K_2O and SiO_2, suggesting severe interference from adjacent minerals. Central portions of large grains give the (Ca+Si)/(Th+U+Pb+S) ratios close to unity. A total of 19 screened data points are arrayed linearly on the PbO versus ThO_2* diagram, and yield an isochron of 164±19 Ma with an intercept value of 0.0004±0.0087 (Fig. 3B).

Huangshan-9: Monazite grains are small and sparse in this sample, and only the 5 grains were available for analysis. As given in Table 2, datasets with Triassic to late Jurassic apparent ages are not uncommon. These data points can be regressed with an isochron of c. 160 Ma (dashed line in Fig. 3C), but they all show large deviation of the (Ca+Si)/(Th+U+Pb+S) ratios from unity. The screened 5 data points define a reliable isochron of 130±19 Ma with an intercept value of -0.0007±0.0116 (Fig. 3C).

Huangshan-10: A total of 15 spots on 5 grains were analyzed, and 9 datasets were selected by the chemical criterion for CHIME age calculation. These data points are arrayed linearly, and yield an isochron of 138±6 Ma with an intercept value of 0.0005±00025 (Fig. 3D).

DISCUSSION AND CONCLUDING REMARKS

Present examination reveals that monazite grains in Wugongshan-2 are chronologically zoned with the central domain of middle Jurassic age and the marginal domain of Cretaceous age, and that the (Ca+Si)/(Th+U+Pb+S) ratio for some spots on transparent clear monazites deviates largely from unity. The chemical criterion that $0.95<(Ca+Si)/(Th+U+Pb+S)<1.05$ discriminates between altered spots and less-altered spots where a closed behavior of the Th-U-Pb system is possibly maintained. The refined CHIME monazite ages are 159±12 Ma and 164±19 Ma for granite samples Wugongshan-2 and 3, respectively. The CHIME monazite ages for granite samples Huangshan-9 and -10 are 130±19 and 138±6 Ma, respectively. Previous CHIME monazite ages, 173±10 Ma for the Wugongshan samples and 162±10 Ma for the Huangshan samples (Suzuki *et al.*, 2000), appear to have resulted from mixing of concordant and discordant datasets and/or datasets for different age domains. Thus, the 173±10 Ma and 162±10Ma age reported by Suzuki *et al.* (2000) are unreliable.

Present study reinforces the middle to late Jurassic age for the granite samples from Wugongshan, 159±12 Ma for Wugongshan-2 K-feldspar porphyritic muscovite-biotite granite and 164±19 Ma for Wugongshan-3 coarse-grained muscovite-biotite granite. The K-feldspar porphyritic and coarse-grained granites occupy the central part of the Wugongshan dome, and are considered to comprise syntectonic bodies (Wang *et al.*, 2001). The middle to late Jurassic K-Ar ages (159–183 Ma) had been given for the granite bodies (JBGMR, 1984). Recent U-Pb dating of zircon yielded 161.0±1.0,

143.8±1.6 and 126.3±6.4 Ma ages for the granitic bodies within the Wugongshan dome (Lou *et al.*, 2005). The 129±14 Ma age for the marginal domains of monazites in Wugongshan-2 agrees well with the 131.7±1.7 Ma $^{40}Ar/^{39}Ar$ age reported by Faure *et al.* (1996) for the margin of the granite body. The revised CHIME monazite ages, 130±19 Ma for Huangshan-9 and 138±6 Ma for Huangshan-10, agree well with each other, and are close to the 125 Ma $^{40}Ar/^{39}Ar$ age reported by Li (2006).

On the basis of the structural analysis and $^{40}Ar/^{39}Ar$ ages (225.6±2.0, 229.0±2.9 and 233.5±5.0 Ma) for metamorphic rocks, Faure *et al.* (1996) suggested a late Triassic age for the ductile deformation and an early Cretaceous age for the final doming in the Wugongshan dome. They considered that most of the metamorphic rocks had been under conditions below 300-400°C since the late Triassic, and regarded the 131.7±1.7 Ma $^{40}Ar/^{39}Ar$ age for the southern margin of the main pluton as the time of the local reworking. The c. 160 Ma CHIME monazite and U-Pb zircon ages possibly date the time of granitic plutonism in the Wugongshan area. The Wugongshan doming is linked with granite emplacement; the F2 fold is due to vertical shortening along the granitic contact (Faure *et al.*, 1996). Incidentally, the F1 fold was considered to be coeval to the main metamorphism on the Indosinian stage. The age of granitic emplacement provides a significant constraint for the development of the extensional environment in the subduction type orogen of southeastern China.

ACKNOWLEDGEMENTS

Drs. Ken Shibata, Iwao Kawabe and Takashi Agata are thanked for the constructive review of the manuscript. Drs. Deyou Sun, Chang-Qing Zheng and Takenori Kato are acknowledged for fruitful discussions. This research was partially supported by the Ministry of Education, Science, Sports and Culture, Grant-in-Aid for Scientific Research (B), No. 19340149, 2007.

REFERENCES

Bence, A.E. and Albee, A.L. (1968): Empirical correction factors for the electron microanalysis of silicates and oxides. *Jour. Geol.*, **76**, 382–403.

Faure, M., Sun, Y., Shu, L., Monié, P. and Charvet, J. (1996): Extensional tectonics within a subduction-type orogen. The case study of the Wugongshan dome (Jiangxi Province, southeastern China). *Tectonophysics*, **263**, 77–106.

JBGMR (Jiangxi Bureau of Geology and Mineral Resources) (1984): Regional geology of Jiangxi province. *Geological Publishing House*, Beijing (China), 921p.

Jiang, Y.H., Qie, J.Z., Liu, H.Y. and Wang, W.G. (1999): A-type granites in Zhejiang-Jiangxi-Anhui provinces, China. *Volcanology and Mineral Resources*, **20**, 48–55.

Kato, T. (2005): New accurate Bence-Albee α-factors for oxides and silicates calculated from the PAP correction procedure. *Geostandards and Geoanalytical Res.*, **29**, 83–94.

Li, X-H. (2000): Cretaceous magmatism and lithosphere extension in Southeast China. *J. Asian Earth Sci.*, **18**, 293–305.

Lou, F.S., Shen, W.Z., Wang, D.Z., Shu, L.Sh. Wu, F.J. Zhang, F.R. and Yu, J.H. (2005): Zircon U-Pb isotopic chronology of the Wugongshan dome compound granite in Jiangxi province. *Acta Geologica Sinica*, **79**, 636–644.

Lou, F.S., Wang, D.Z., Shu, L.Sh. and Yu, J.H. (2006): Discussion on the genesis of metamorphic core complex related to magmatic termo-uplift in Wugongshan. In: J. Chen (Ed.), *Research*

Progress on Geology and Geochemistry. Nanjing University Press, Nanjing (China). pp. 146–156.

Pearce, J.A., Harris, N.B.W. and Tindle, G.A. (1984): Trace element discrimination diagrams for the tectonic interpretation of granitic rocks. *J. Petrol.*, **25**, 956–983.

Smellie, J.A.T., Cogger, N., Herrington, J. (1978): Standards for quantitative microprobe determination of uranium and thorium with additional information on the chemical formulae of davidite and euxenite-polycrase. *Chem. Geol.*, **22**, 1–10.

Sun, D.Y. and Suzuki, K. (2004): CHIME dating of granites exposed in the Huanggoushan area of the Julin province, China. *Bull. Nagoya Univ. Museum*, No. 20, 15–23.

Suzuki, K. and Adachi, M. (1991): Precambrian provenance and Silurian metamorphism of the Tsubonosawa paragneiss in the South Kitakami terrane, Northeast Japan, revealed by the chemical Th-U-total Pb isochron ages of monazite, zircon and xenotime. *Geochemical J.*, **25**, 357–376.

Suzuki, K., and Adachi, M. (1998): Denudation history of the high T/P Ryoke metamorphic belt, Southwest Japan: constraints from CHIME monazite ages of gneisses and granitoids. *Jour. Metamorphic Geol.*,**16**, 23–37.

Suzuki, K. and Kato, T. (in press): CHIME dating of monazite, xenotime, zircon and polycrase: protocol, pitfalls and chemical criterion of possibly discordant age data. Gondwana Research.

Suzuki, K., Karakida, Y. and Kamada, Y. (2000): Provenance of granitic anchor stones recovered from the Takashima submerged site: an approach using the CHIME method for dating of zircons. *Proc. Japan Acad.*, **76**, 139–144.

Wang, D.Z., Shu, L.Sh., Faure, F. and Sheng, W.Z. (2001): Mesozoic magmatism and granitic dome in the Wugongshan Massif, Jiangxi province and their genetical relationship to the tectonic events in southeast China. *Tectonophysics*, **339**, 259–277.

Whalen, J.B., Currie, K.I. and Xhappell, B.W. (1987): A-type granites: geochemical characteristics, discrimination and petrogenesis. *Contrib. Mineral. Petrol.*, **95**, 407–419.